

KfK 5404
ANL-94/36
November 1994

Conceptual Design of a Forced-Flow-Cooled 20-kA Current Lead Using Ag- Alloy-sheathed Bi-2223 High-Temperature Superconductors

R. Heller, J. R. Hull
Institut für Technische Physik
Projekt Kernfusion

Kernforschungszentrum Karlsruhe

KERNFORSCHUNGSZENTRUM KARLSRUHE

**Institut für Technische Physik
Projekt Kernfusion**

KfK 5404

ANL-94/36

CONCEPTUAL DESIGN OF A FORCED-FLOW-COOLED 20-KA CURRENT LEAD USING AG-ALLOY-SHEATHED BI-2223 HIGH-TEMPERATURE SUPERCONDUCTORS

R.Heller, J.R. Hull*

***Argonne National Laboratory
Energy Technology Division
Argonne, IL, 60439
USA**

Kernforschungszentrum Karlsruhe GmbH, Karlsruhe

Als Manuskript gedruckt
Für diesen Bericht behalten wir uns alle Rechte vor

Kernforschungszentrum Karlsruhe GmbH
Postfach 3640, 76021 Karlsruhe

ISSN 0303-4003

Abstract

The use of high-temperature superconductors in current leads to reduce refrigeration power has been investigated by many groups in the past. Most used YBCO and Bi-2212 bulk superconductors, although their critical current density is not very high. In this paper, Bi-2223 HTSC tapes sheathed with Ag alloys are used in the design of a 20-kA current lead because of their higher critical current in medium magnetic fields. The lead current of 20 kA is related to the coil current of the planned stellarator WENDELSTEIN 7-X. Forced-flow helium cooling has been used in the design, allowing position-independent and well-controlled operation. The design characteristics of the lead are presented and 4-K helium cooling of the whole lead, as well as 60-K helium cooling of the copper part of the lead, is discussed. The power consumption at zero current, and the lead's behaviour in case of loss of coolant flow, are given. The results of the design allow extrapolation to current leads of the 50-kA range.

Konzeptioneller Entwurf einer zwangsgekühlten 20-kA Stromzuführung unter Verwendung von mit einer Silberlegierung verstärkten Bi-2223 Hochtemperatursupraleitern

Zusammenfassung

Die Verwendung von Hochtemperatursupraleitern in Stromzuführungen zur Reduzierung der Kühlleistung wurde in der Vergangenheit bereits von verschiedenen Gruppen untersucht. Die meisten benutzten YBCO bzw. Bi-2212 Bulk-Material, obwohl deren kritische Stromdichte nicht sehr hoch war. In diesem Bericht werden für den Entwurf einer 20-kA Stromzuführung Bi-2223 Bänder verwendet, die mit einer Silberlegierung verstärkt sind. Der Grund liegt in der höheren kritischen Stromdichte bei 77 K in magnetischen Hintergrundfeldern von bis zu 0.5 Tesla. Der gewählte Strom der hier betrachteten Stromzuführung ist dem Spulenstrom des geplanten Stellarators Wendelstein 7-X angepaßt. Heliumzwangskühlung wird in diesem Design verwendet, weil sie lageunabhängigen und kryotechnisch gut kontrollierbaren Betrieb ermöglicht. In diesem Bericht werden die Eigenschaften der Stromzuführung beschrieben sowie 4-K bzw. 60-K Heliumkühlung untersucht. Die Kühlleistung im Null-Stromfall sowie die Eigenschaften der Stromzuführung bei Ausfall des Kühlmittelflusses werden diskutiert. Die Ergebnisse des Entwurfs erlauben eine Extrapolation zu Stromzuführungen im 50-kA Bereich.

Contents

- 1.0 Introduction 1**
- 2.0 Conceptual design 4**
- 3.0 Cooling concept 10**
- 4.0 Calculation results 11**
 - 4.1 General 11
 - 4.2 4-K Helium cooling 12
 - 4.3 60-K Helium cooling 16
 - 4.4 Refrigeration power consumption 20
 - 4.5 Effect of contact resistance at 4-K and 60-K levels 23
 - 4.6 Effect of higher temperature of HTSC part 24
- 5.0 Transient behaviour in case of loss of helium mass flow 26**
- 6.0 Summary and conclusions 30**
- 7.0 References 32**

Figures

1.	Thermal conductivity of various HTSC materials, of Ag-Au-alloys, and of phosphorous-deoxidized copper	2
2.	Heat capacity of various HTSC materials and of Cu, Ag, and Au	2
3.	Critical current density of various HTSC materials vs. applied magnetic field at 77 K	3
4.	Sketch of HTSC current lead	4
5.	Cross section of HTSC part of lead	5
6.	Magnetic self field of HTSC part at 20 kA	6
7.	Critical current vs. magnetic field and load line of HTSC part at 77 K	7
8.	Current-sharing temperature vs. operation current of HTSC part	8
9.	Vertical cut through HTSC part including connection regions	9
10.	Sketch of cooling concepts of HTSC current lead	10
11.	Temperature profiles of HTSC current lead for 4-K-He cooling and 0, 16 and 20 kA	12
12.	Helium mass flow rate vs. current for 4-K He cooling concept	14
13.	Helium mass flow rate normalized to current vs. current for 4-K He cooling concept	14
14.	Voltage drop vs. current for 4-K He cooling concept	15
15.	Temperature at upper end of HTSC part and maximum temperature difference between HTSC and helium vs. current for 4-K He cooling concept	15
16.	Temperature profiles of HTSC current lead for 60-K He cooling and 0, 16 and 20 kA	16
17.	Helium mass flow rate vs. current for 60-K He cooling concept	18
18.	Helium mass flow rate normalized to current vs. current for 60-K He cooling concept	18
19.	Voltage drop vs. current for 60-K He cooling concept	19
20.	Temperature at upper end of HTSC part and maximum temperature difference between Cu and helium vs. current for 60-K He cooling concept	19
21.	Total power consumptions for the HTSC and the combined leads at different currents	21
22.	Reduction factor for the HTSC lead for both cooling concepts at different currents	22
23.	Temperature profiles of HTSC current lead for 60-K He cooling and various temperature at the upper end of HTSC part	25
24.	Temperature profiles of HTSC lead at 20 kA at various times after switching off helium mass flow (4-K He cooling)	27
25.	Temperature profiles of HTSC lead at 20 kA at various times after switching off helium mass flow (60-K He cooling)	27
26.	Temperature profiles of HTSC lead at 20 kA without Ag-alloy stabilizer after switching off helium mass flow (4-K He cooling)	28
27.	Time-of-danger and temperature at coil side (bottom temperature) of HTSC lead at 20 kA after switching off mass flow (4-K He cooling)	29
28.	Temperature profiles of HTSC lead at 20 kA for different Ag-alloy stabilizer cross sections at the burn-out time (4-K He cooling)	30

Tables

1.	Input parameters of heat exchanger for proposed HTSC current lead	11
2.	Heat loads at 4-K and 60-K level for different currents for 4-K He cooling (version 1) . . .	13
3.	Heat loads at 4-K resp. 60-K level for different currents for 60-K He cooling (version 2) . . .	17
4.	Recooling and refrigeration rates for various current leads	20
5.	Heat loads at 4-K resp. 60-K level for different currents for 60-K He cooling (version 2) . . .	23
6.	Comparison of current leads with different temperatures at the upper end of HTSC part for 60-K He cooling	24

1.0 Introduction

The use of high-temperature superconductors (HTSCs) in current leads to reduce the refrigeration power necessary to operate a superconducting magnet has been investigated by many groups in the past. The reasons are the high critical temperature and the low thermal conductivity of the HTSC material. Theoretical studies result in a refrigeration power that is lower by a factor of five than that of a conventional copper lead. These studies assume a heat sink at 77 K and make use of the higher efficiency of a cooling machine operating between 77 K and room temperature. The heat sink can be realised by using either a liquid nitrogen bath at the transition region between the HTSC and the copper part of the lead or helium gas at high pressure. Both solutions lead to a similar refrigeration power, i.e., to a similar reduction with respect to a conventional lead [1], [2]. The consequence is that the decision of whether to use LN₂ or helium gas at high pressure depends on the boundary conditions of the experimental facility, i.e., the kind of refrigerator.

Most of the investigations concentrated on the use of bulk HTSC, i.e., YBCO or Bi-2212. Several prototypes of current leads of the 1 - 2 kA class have been designed and tested [3-5]. The results were encouraging although the refrigeration power was not as low as given above. The reason is that the real heat load at 4 K is due not only to heat conduction; one must add the contact losses from the HTSC part to the superconducting coil which is in the same order of magnitude as the HTSC heat load.

The disadvantages of the bulk material are:

- Low critical current density even at zero applied magnetic field: A critical current density of the superconductor of 6 - 9 A/mm² at zero applied magnetic field and about 1 A/mm² at 80 mT is reported [6].
- High thermal instability in case of fault conditions, e.g. loss of cooling [2,7].

To overcome these problems, the suggestion was made to use HTSC material that has been electrically and mechanically stabilized by a metal, i.e., silver or silver alloy. The higher thermal conductivity of that material could be balanced by using longer lengths of the material. Geometrically, these are no longer bulk material but tapes or wires consisting of a core made of Bi-2223 or Bi-2212 HTSC and a silver or silver-alloy sheath. An interesting development has been given in [8,9]. This group uses silver-gold alloys which have thermal conductivities comparable to that of phosphorous-deoxidized copper, i.e., several orders of magnitude lower than that of pure silver. The critical current density of the superconductor reported is 25 A/mm² at zero applied magnetic field and 11 A/mm² at 80 mT. This is a factor of 4 higher than for the Bi-2212 bulk material at zero field resp. a factor of 11 higher at 80 mT. Bi-2223 tapes with Ag-Mg-alloy sheath have even higher critical current densities [10,11].

Figure 1 shows the thermal conductivities of various HTSC materials and of Ag-Au-alloy and phosphorous-deoxidized copper. In Figure 2, the heat capacities of HTSC materials, copper, silver, and gold have been plotted as a function of temperature.

Figure 3 shows the critical current density of various HTSC materials as a function of applied magnetic field at 77 K. The numbers were deduced from measurement data given in [10], which are compatible to results obtained from samples with long lengths, i.e., 0.5 m [11].

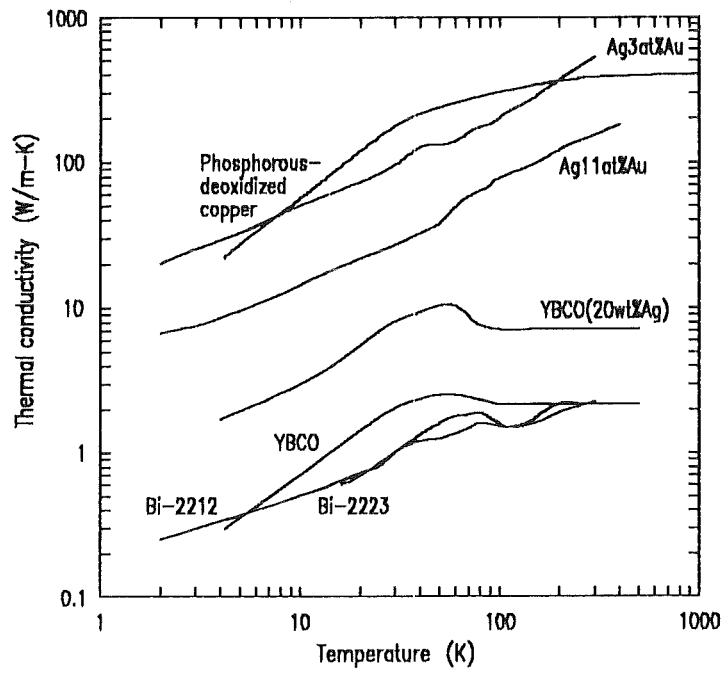


Figure 1. Thermal conductivity of various HTSC materials, of Ag-Au-alloys, and of phosphorous-deoxidized copper

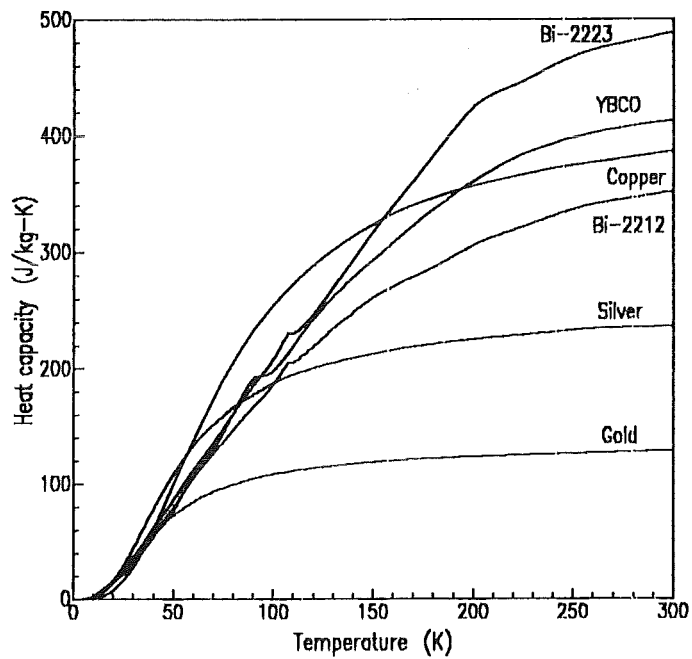


Figure 2. Heat capacity of various HTSC materials and of Cu, Ag, and Au

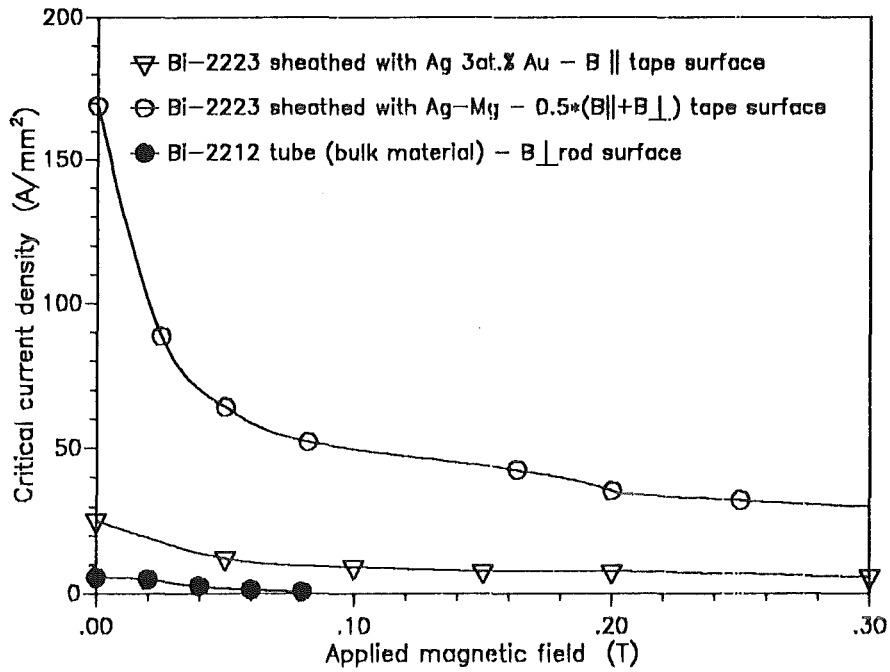


Figure 3. Critical current density of various HTSC materials vs. applied magnetic field at 77 K

It should be mentioned that the critical current densities of the Bi-2223 tapes sheathed with Ag-Mg are average values for both parallel and perpendicular applied magnetic field directions. This has been done to obtain numbers applicable for the design described in the next chapter. It is acceptable to assume that critical current densities for the Bi-2223 tapes sheathed with Ag-Au-alloy could be as high as for the ones sheathed with Ag-Mg.

This behaviour led to the decision to use Bi-2223 sheathed with Ag 3 at.% Au alloy for the conceptual design of a 20-kA current lead cooled with forced-flow helium. The use of 3 at.% Au in the Ag-alloy is somehow arbitrary, but does not affect the conceptual design, especially the length of the HTSC part. The current of 20 kA has been chosen to make a design feasible for application to the planned stellarator WENDELSTEIN 7-X [12].

2.0 Conceptual design

The conceptual design of a 20-kA current lead must fulfill the following requirements:

- low thermal load on 4-K level
- low contact losses on both 4-K and 70-K level
- high thermal stability with respect to loss of coolant flow
- mechanical rigidity

The current lead can be divided into five parts, i.e.:

1. copper heat exchanger,
2. HTSC part,
3. 70-K transition between copper and HTSC part,
4. 4-K transition between HTSC part and coil connection, and
5. connection to superconducting coil.

A sketch of the lead is given in Figure 4.

In version 1, the lead is cooled by 4-K helium at high pressure whereas in version 2, the lead is cooled by 60-K helium.

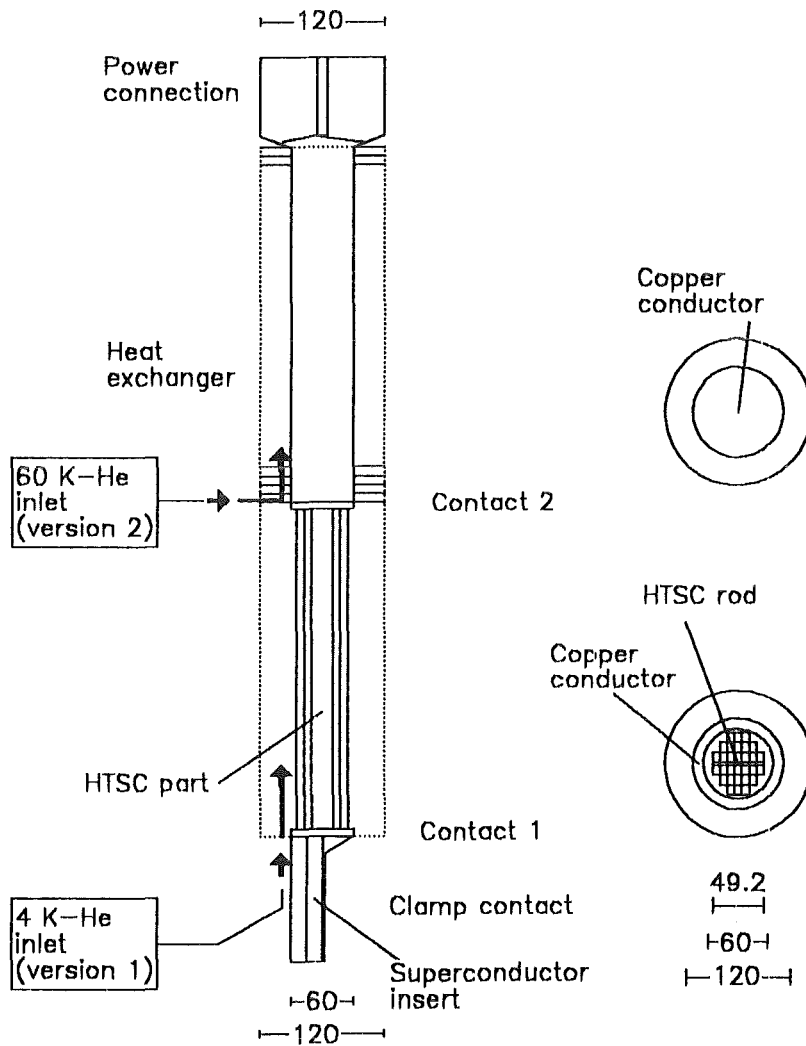


Figure 4. Sketch of HTSC current lead. Dimensions are given in mm

The design of the copper heat exchanger is similar to that of the combined copper Nb₃Sn current lead [13], i.e., a central conductor made of phosphorous-deoxidized copper carrying the current and surrounded by perforated copper plates that are brazed onto the copper rod to form the heat exchanger. The radial dimension of the copper conductor is maintained by the outer dimension of the HTSC part. For technical reasons, the perforated copper plates must be mounted from the lower end of the copper conductor. This means that the inner diameter of the plates must be as large as the largest radial extension of the HTSC part because no clamping or screwing should be made in the transition region between the copper and the HTSC part. This results in a diameter of the conductor of 60 mm, leading to a current density at 20 kA of 7.07 A/mm² (for comparison: the current density in the POLO lead at 30 kA is 7.8 A/mm²). The conductor diameter of the current lead proposed for W 7-X (see [14]) is 55 mm, leading to a current density at 20 kA of 8.4 A/mm².

The connection to the superconducting coil will be done by clamping - as done for the 30 kA lead [13] - and the conductor is now made of electrolyte touched copper (E-copper). The clamp contact has a length of 300 mm, leading to a surface current density at 20 kA of 1.11 A/mm². Due to the large dimension of the clamp contact, electrical resistance would be ≈ 25 n Ω . Therefore, it has been decided to equip the copper conductor with an Nb₃Sn insert, as done for the POLO lead [15]. This reduces the resistance significantly. Based on measurements done for the POLO lead - which has phosphorous-deoxidized copper in the contact region - an electrical resistance of ≈ 2 n Ω should be possible with E-copper.

For the same reasons, the connection between the HTSC part and the copper heat exchanger will be made of E-copper. At 77 K, the electrical resistivity of copper with an residual resistivity ratio (RRR) of 50 is a factor of 2.5 less than the corresponding one with an RRR of 5. So that thermal - and electrical - contact is as good as possible, the connection part will be friction-welded to the copper conductor of the heat exchanger which is made of phosphorous-deoxidized copper.

The HTSC part has been realized by stacking Bi-2223 tapes. Each tape has a cross section of 8 mm x 0.3 mm, the superconductor fraction is 0.65, the stabilizer is made of silver with 3 at.% Au to reduce thermal conductivity, as proposed in [8,9]. A total of 27 tapes are stacked to form a so-called "module" of 8 mm x 8.1 mm cross section. The length of the module is a parameter that must be adjusted during optimization of the whole lead, together with the length of the copper heat exchanger. This will be described later. To get well-defined conditions at both ends, sockets made of the same Ag alloy will be rolled to the ends. ("Well-defined conditions" means good soldering and good calibration of cross-sectional and axial dimensions). Afterwards, the module will be heat treated. The final cross-sectional dimension is 8.2 mm x 8.2 mm. For the 20-kA lead, 28 modules are needed. These are put together to form a rigid rod, as shown in Figure 5. The current density in superconductor at 20 kA is then 17 A/mm². Around the rigid rod, a sheet made of stainless steel will be wrapped.

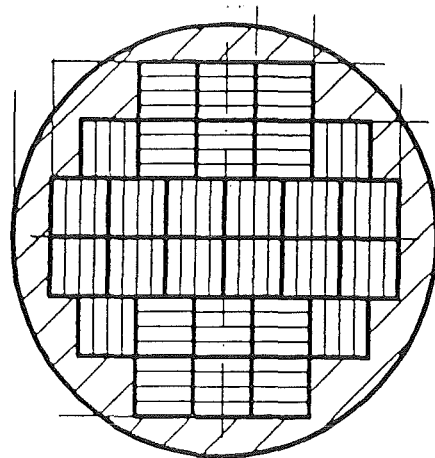


Figure 5. Cross section of HTSC part of lead

Due to the strong dependence of the critical current density of the HTSC tapes on the magnetic field, the self field of the HTSC part has been calculated by the computer code EFFI [16]. At 20 kA, the maximum magnetic self field is 0.16 T. Figure 6 shows a contour plot of the HTSC part and the magnetic field vs. radial dimension cut in the center.

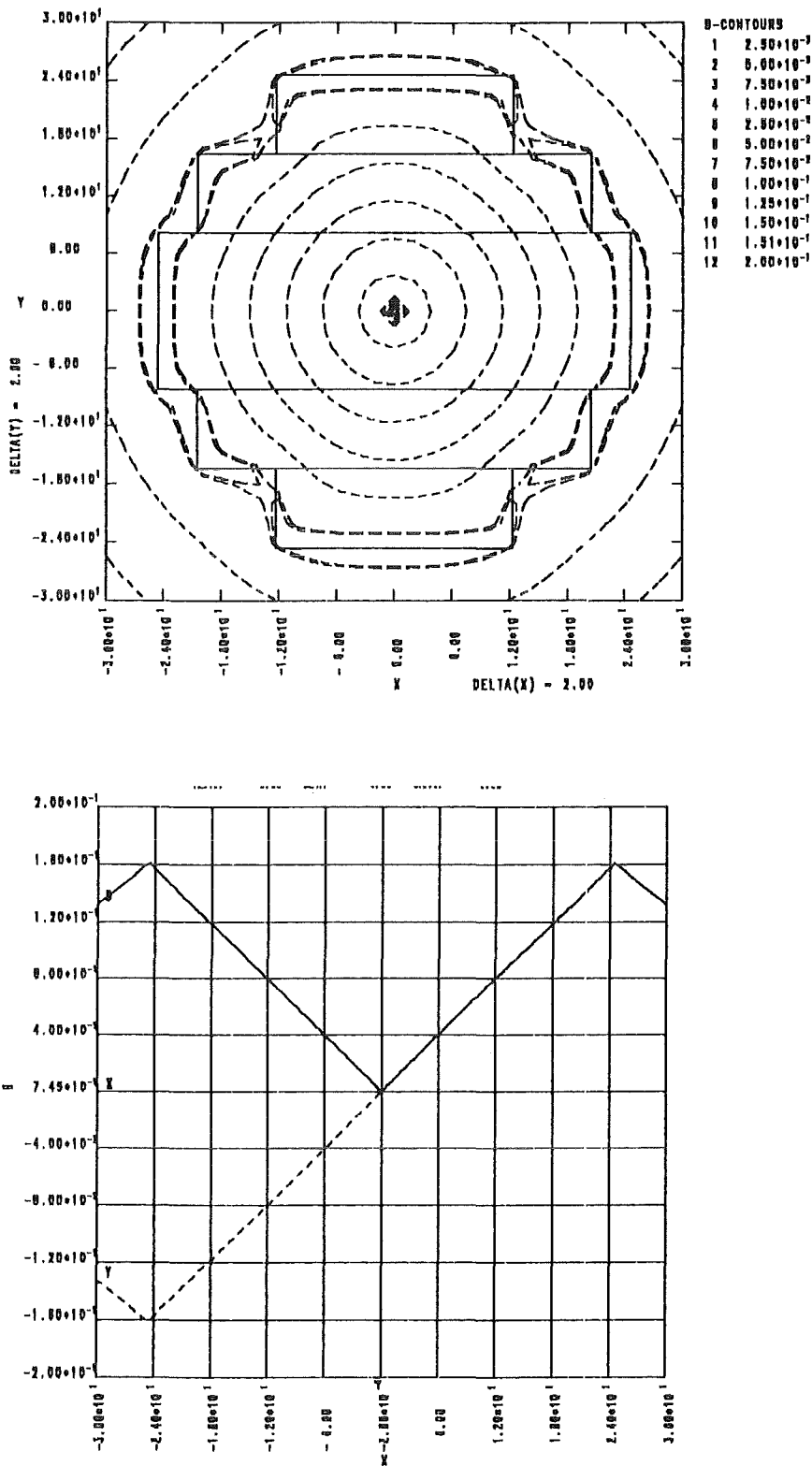


Figure 6. Magnetic self field of HTSC part at 20 kA.
 Top: contour plot in radial plane of HTSC part.
 Bottom: Field vs. radial dimension in center of HTSC part.

For the design, a magnetic background field of 0.25 T at a current of 20 kA has been assumed, taking into account an additional background magnetic field of about 0.1 T from the superconducting coil. Following an idea given in [17], the modules have been aligned so that the applied magnetic field is as parallel to the tape surface as possible. In the calculations, it was assumed that the magnetic field is an average of the field parallel and perpendicular to the tape surface. Figure 7 shows the critical current of the HTSC part as a function of applied magnetic field, as been derived from the critical current density of Bi-2223 tapes (see Figure 3). The load line of the HTSC part has also been plotted. It is seen that in nominal operation, the critical current is roughly a factor of 2 higher than the operation current. In Figure 8, the current-sharing temperature T_{cs} , i.e., the temperature at which the operation current is as high as the critical current, is plotted as a function of the operation current. The maximum operation temperature of the HTSC part of the lead is also indicated.

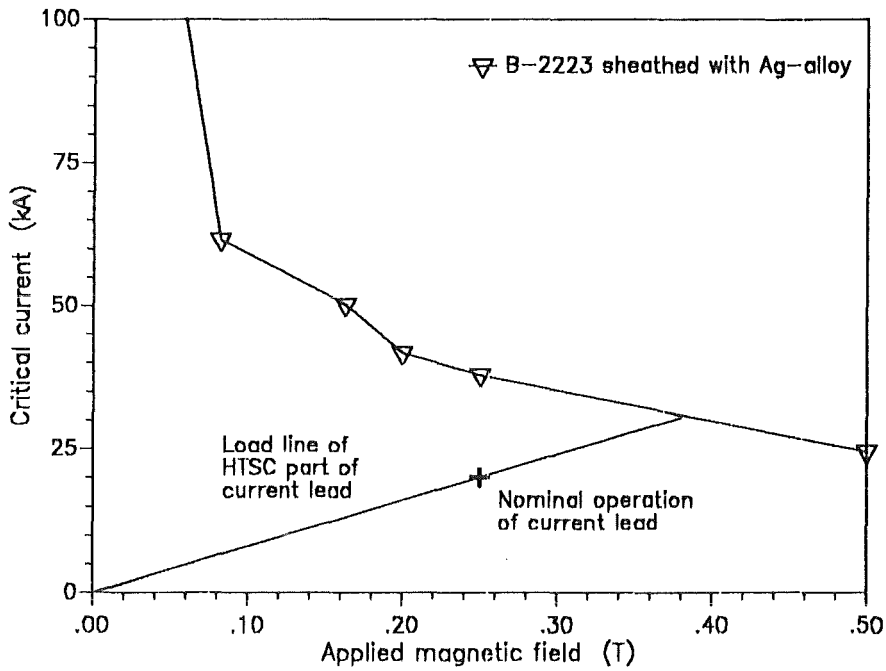


Figure 7. Critical current vs. magnetic field and load line of HTSC part at 77 K

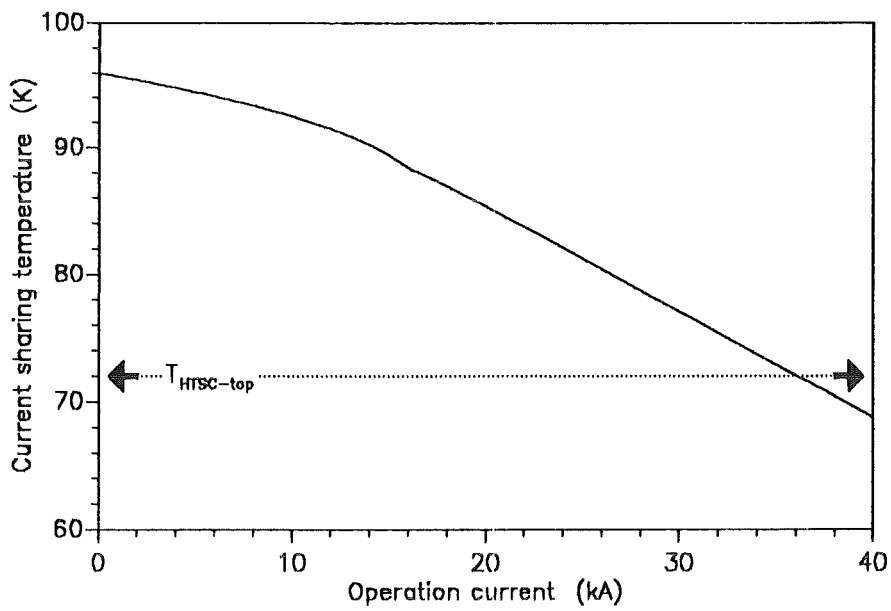


Figure 8. Current-sharing temperature vs. operation current of HTSC part

The connections of the HTSC part to the copper heat exchanger as well as the clamp contact to the coil will be done by soft-soldering because neither welding nor brazing is allowed due to their high temperatures. Because of space restrictions, clamping is also not permitted.

The connections will be done as follows:

1. Grooves will be cut in the copper of the connection part which must fit the lateral dimension of the HTSC part.
2. The HTSC rod will be soldered in the grooves.

Electrical resistances for the soldered connection of $2.5 \text{ n}\Omega$ at 4 K and $15 \text{ n}\Omega$ at 77 K should be possible. These numbers are used in the calculations shown later.

Figure 9 shows a vertical cut through the HTSC part, including the connection regions.

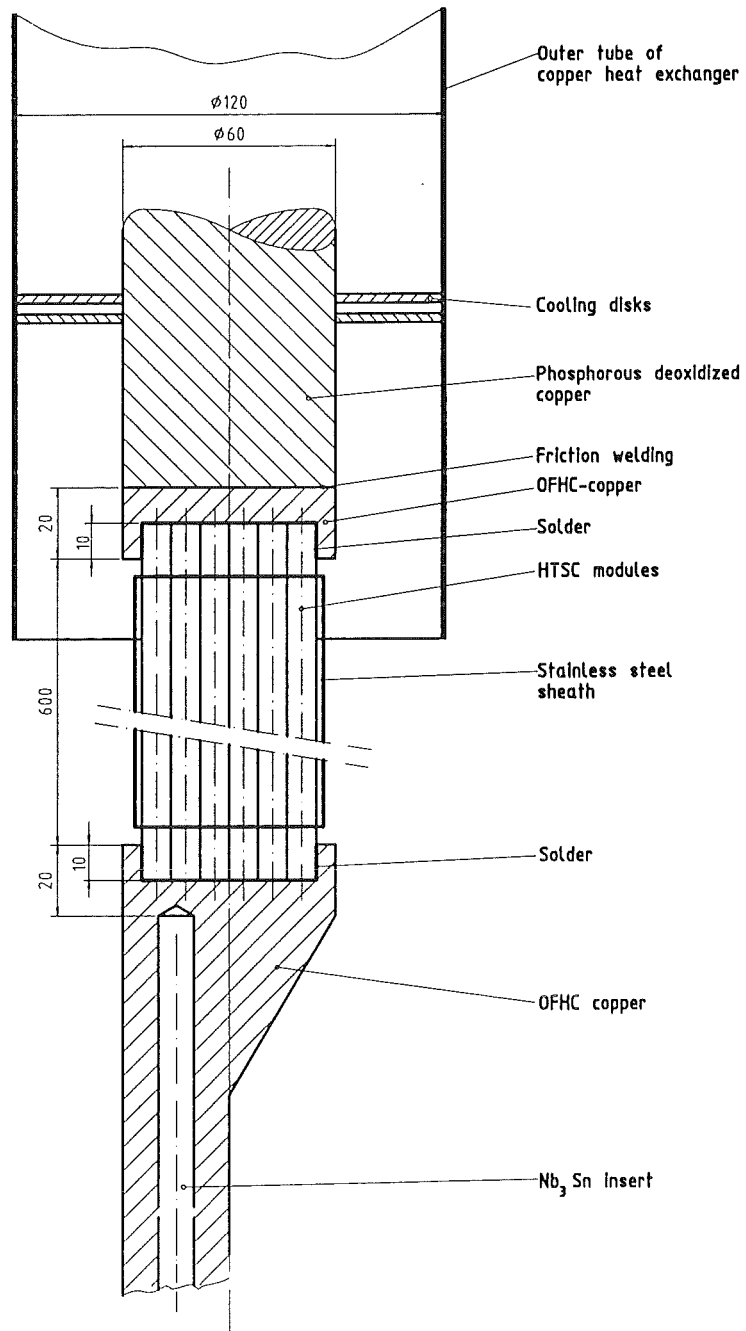


Figure 9. Vertical cut through HTSC part including connection regions. Dimensions given in mm are those used in the calculations and do not represent an engineering design.

3.0 Cooling concept

As already mentioned, two different cooling concepts will be discussed and compared to the conventional current lead cooling:

- 4-K He cooling and
- 60-K He cooling.

Both cooling concepts require different designs, i.e.,

- length of the copper heat exchanger and
- arrangement of cooling inlet.

In the 4-K He cooling, the inlet will be at the connection region, pointing toward the superconducting coil. In Figure 4, the inlet is marked with "version 1."

In the 60-K He cooling, the inlet will be either at the connection region between the HTSC and copper parts (marked with "version 2") or at the coil side. The first possibility requires radial access from the outside, i.e., vacuum region of the cryostat, and one must penetrate the insulation vacuum which is located around the heat exchanger of the lead to reduce radial heat load. The second possibility requires a thermally insulated pipe entering the lead at the connection region between the lead and the coil and bypassing the HTSC part. In both cases, there must be a vacuum-tight plate just above the HTSC part because the space around this part should be in vacuum.

In Figure 10, the three versions are sketched.

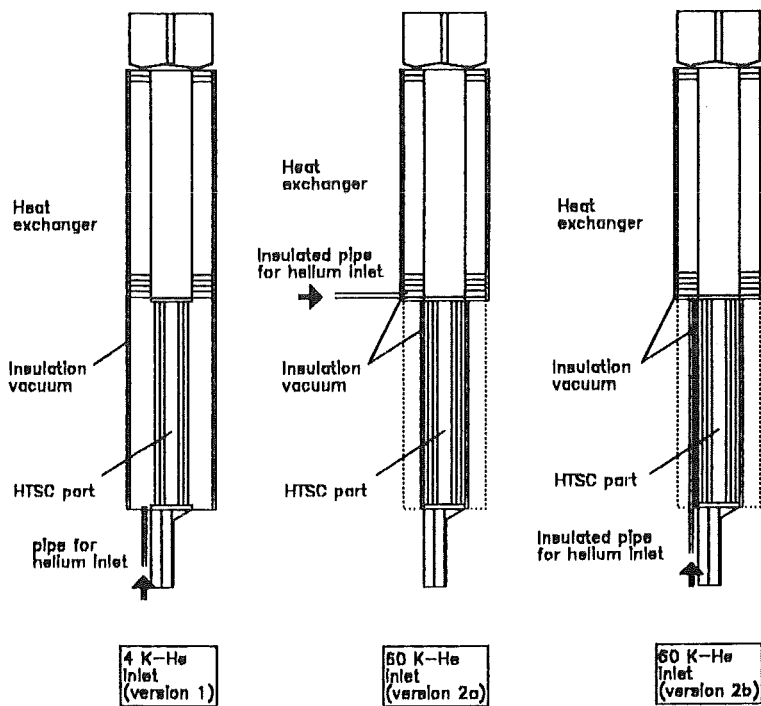


Figure 10. Sketch of cooling concepts of HTSC current lead.

- left: 4-K He cooling.
center: 60-K He cooling (radial).
right: 60-K He cooling (axial).

4.0 Calculation results

4.1 General

The calculations were done using the computer code CURLEAD [18,19].

In Table 1, the main parameters of the HTSC current lead are summarized. Version 1 denotes the 4-K He cooling concept, version 2 the 60-K He cooling concept.

Parameter	Unit	Value	
		HTSC part	Copper part
Heat exchanger type	-	rectangular rods	central conductor surrounded by perforated copper plates
Length	m	0.66	0.50 (version 1) 1.35 (version 2)
Cross section of conductor	cm ²	18.14	28.27
Fraction of superconductor	-	0.65	n.a.
Cooled perimeter of heat exchanger P_{cool}	m	0.18	9.27
Cross section of helium A_{He}	cm ²	n.a.	31.5
RRR of cooling disks	-	n.a.	50
Rib efficiency of cooling disks	-	n.a.	function of temperature
Cross-sectional dimensions of HTSC rod	mm x mm	8 x 8.1	n.a.
Number of HTSC rods		28	n.a.
Total length of lead (including ends)	m	1.80 (version 1) 2.65 (version 2)	
Helium inlet temperature	K	4.50	
Helium inlet pressure	MPa	0.40	
Conductor temperature at low-temperature end	K	5.0	
Conductor temperature at upper end of HTSC part	K	<72	
Conductor temperature at high-temperature end	K	285 - 295	

Table 1. Input parameters of heat exchanger for proposed HTSC current lead. Version 1 denotes 4-K He cooling; version 2 60-K He cooling. n.a. = not applicable.

4.2 4-K Helium cooling

First, the current lead has been optimized for 4-K He cooling by adjusting the length of the copper heat exchanger and the HTSC part for a maximum current of 20 kA. The procedure used is described in [7]. The results are as follows:

$$\begin{aligned} L_{\text{copper}} &= 0.50 \text{ m} \\ L_{\text{HTSC}} &= 0.66 \text{ m} \\ L_{\text{total}} &= 1.80 \text{ m (incl. ends)} \\ \dot{m} &= 0.69 \text{ g/s} \end{aligned}$$

The conductor temperature at the coil end was fixed at 5 K, and the helium temperature was 4.5 K. Conductor temperature at the warm end with Neumann condition $dT/dx=0$ was 295 K, and the corresponding helium temperature was 290 K. The upper end of the HTSC part was at 66 K. Due to poor cooling of the HTSC part of the lead, the largest temperature difference between the current-carrying part and the coolant was about 60 K, at the upper end of the HTSC part. At lower currents, i.e., below 20 kA, the current lead is not optimized because of the fixed length of the copper conductor.

In Figure 11, the conductor temperature along the current lead is plotted for different currents.

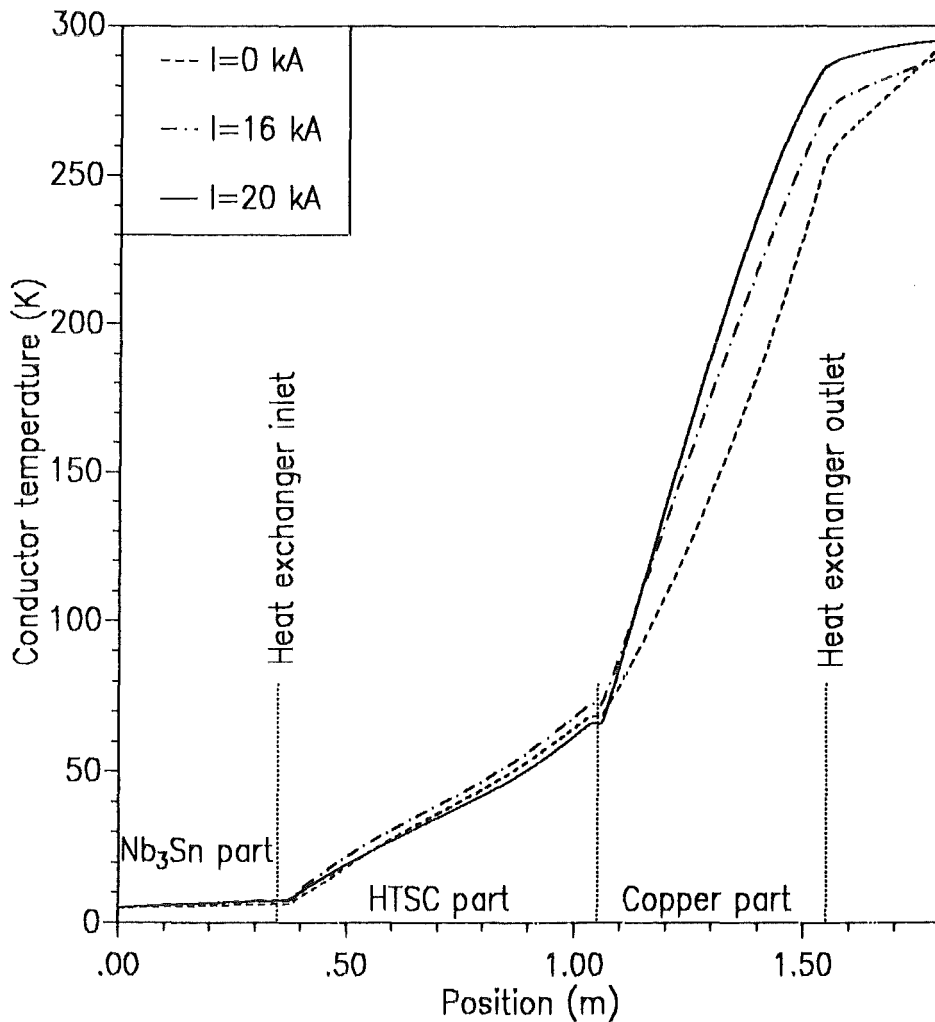


Figure 11. Temperature profiles of HTSC current lead for 4-K-He cooling and 0, 16 and 20 kA

There are several conclusions:

- At 20 kA, no heat is conducted toward or out of the warm end of the lead, i.e., the optimization is fulfilled.
- At lower currents, and moreover at zero current, there is a positive temperature gradient at the warm end, resulting in heat flowing toward the lead (i.e., the lead is too short). This leads to a mass flow rate that is higher than for an optimized lead at that current.
- Due to the 4-K He cooling, the temperature at the upper end of the HTSC part is not fixed.
- The heat load at the connection region between the HTSC part and the superconducting coil is the sum of the thermal conduction from the HTSC part and the resistive heat of the contact. Therefore, heat load at this location depends on the current.
- The heat load at the connection region between the HTSC part and the copper heat exchanger is the sum of the thermal conduction from the copper heat exchanger and the resistive heat of the connection. Therefore, heat load here also depends on current. Due to the large temperature difference between the conductor and the helium at the upper end of the HTSC part and the lower end of the copper heat exchanger, the heat load at that location can be partly transferred to the coolant and not conducted to the 4-K level of the lead.

As an example for the 20-kA run: A heat load of about 325 W is conducted from the copper heat exchanger, but only 12.6 W are transferred to the HTSC part of the lead. Most of the heat (i.e., about 95%) is taken by the helium at the lower part of the copper heat exchanger. At the HTSC part, a heat transfer coefficient of about 3.5 W/m²-K has been obtained; a cooled perimeter of 0.18 m leads to a heat transfer of 0.63 W/m-K · 60 K = 37.8 W/m. This must be compared to a resistive heat of 5.3 W plus a thermal conduction load of 7.3 W, for a total of 12.6 W; i.e.; for a constant temperature difference of 60 K, one needs a length of 30 cm to transfer the heat to the helium.

In fact, the temperature difference decreases, and one needs a longer length. In this example, 3.3 W of the 12.6 W are conducted toward the superconducting coil because there is a balance between heat transfer and heat conduction due to the temperature gradient along the HTSC part of the lead.

Table 2 summarizes the heat-load results for the different currents. It should be mentioned that in these calculations only DC operation has been investigated. No AC losses e.g. due to ramping has been studied.

Current [kA]	4-K level		60-K level	
	Q _{Resi} [W]	Q _{Cond} [W]	Q _{Resi} [W]	Q _{Cond} [W]
0	0.0	2.30	0.0	7.30
6.7	0.21	3.00	0.69	11.51
13	0.79	3.68	2.54	9.98
16	1.17	4.27	4.14	9.36
20	1.87	3.29	5.29	7.25

Table 2. Heat loads at 4-K and 60-K level for different currents for 4-K He cooling (version 1)

Figures 12 - 15 show the helium mass flow rate, the mass flow rate normalized to current, the voltage drop, and the maximum temperature of the HTSC as well as the maximum temperature difference between HTSC part and helium at the HTSC part as a function of current. For comparison, the numbers for the W 7-X combined lead are also plotted. It is clearly seen that the HTSC lead is optimized for a fixed current, whereas the W 7-X lead has a variable length (e.g. see Figure 13). The difference in mass flow rate between the combined and the HTSC lead shrinks for lower currents. The temperature of the HTSC at the upper end of the HTSC part is not fixed but varies between 65 K and 71 K. In the same way, the temperature difference between the HTSC and the helium varies; the helium temperature at the upper end of the HTSC part is about 6.5 K.

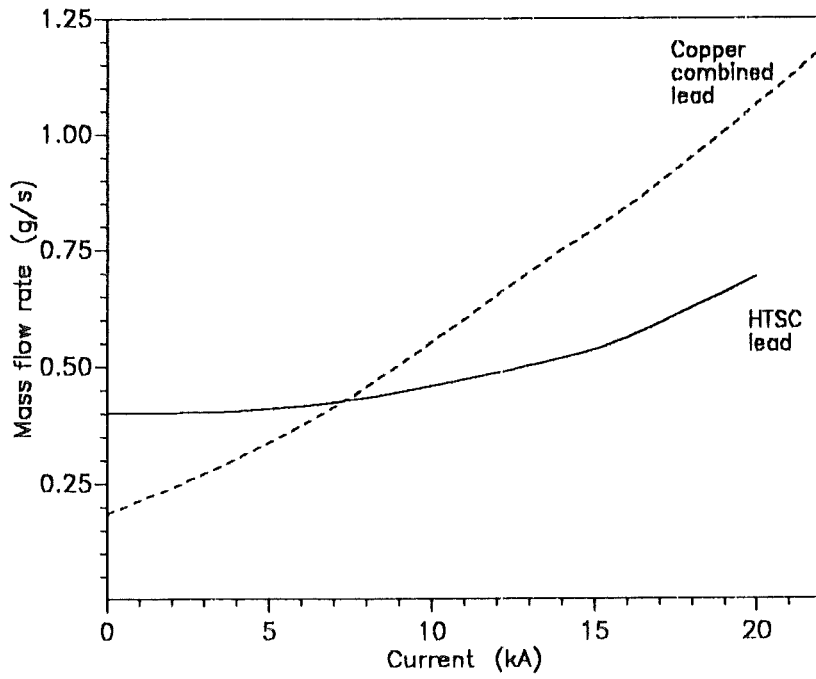


Figure 12. Helium mass flow rate vs. current for 4-K He cooling concept. The dashed line represents the calculation results for the 16 - 20 kA Nb₃Sn combined lead as proposed for W 7-X

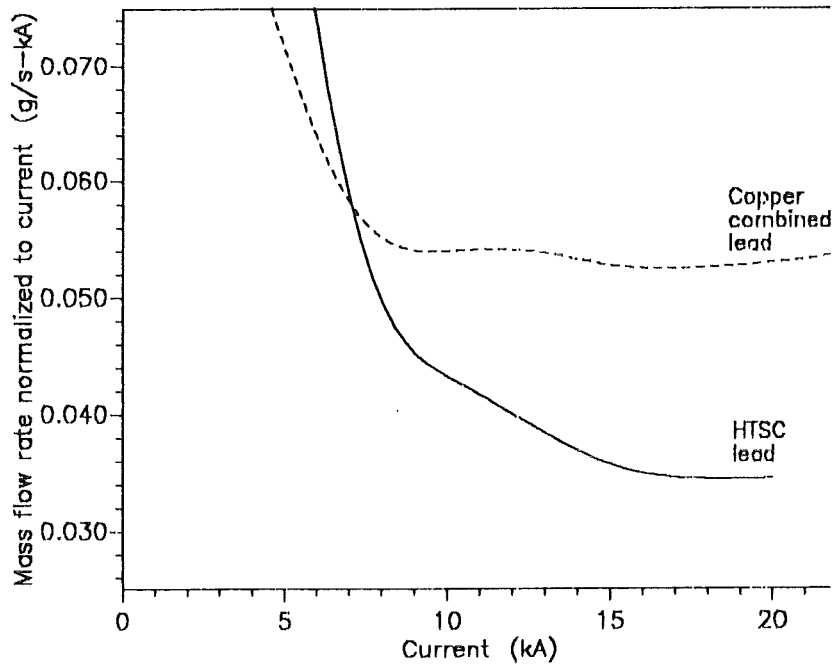


Figure 13. Helium mass flow rate normalized to current vs. current for 4-K He cooling concept. The dashed line represents the calculation results for the 16 - 20 kA Nb₃Sn combined lead as proposed for W 7-X

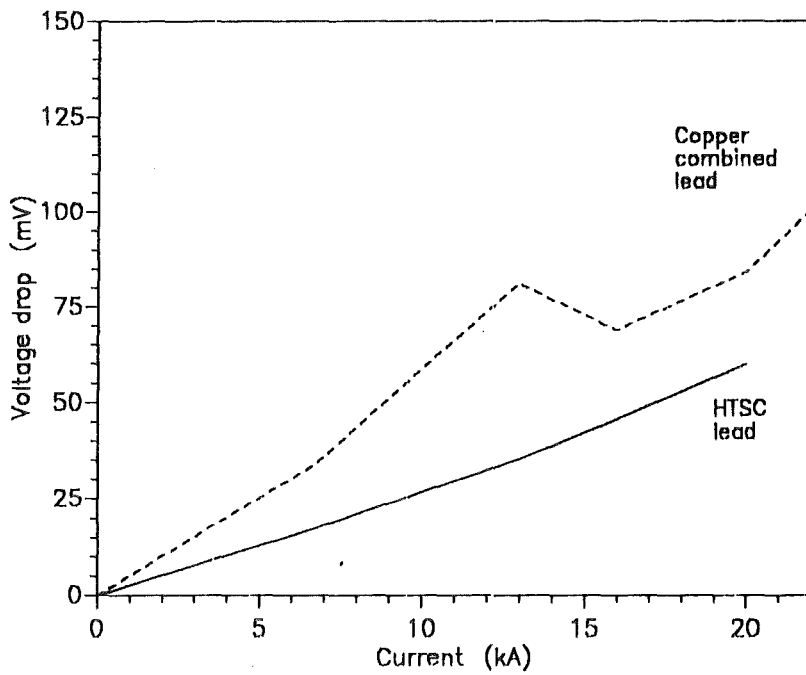


Figure 14. Voltage drop vs. current for 4-K He cooling concept. The dashed line represents the calculation results for the 16 - 20 kA Nb₃Sn combined lead as proposed for W 7-X

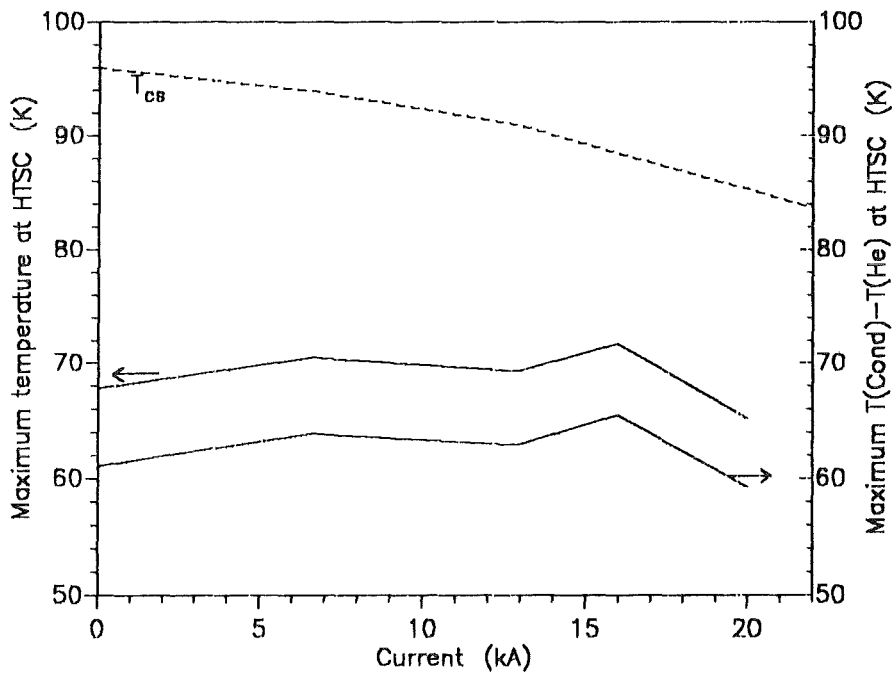


Figure 15. Temperature at upper end of HTSC part and maximum temperature difference between HTSC and helium vs. current for 4-K He cooling concept

4.3 60-K Helium cooling

Second, the current lead has been optimized for 60-K He cooling by adjusting the length of the copper heat exchanger and the HTSC part for a maximum current of 20 kA. The procedure is the same as for the 4-K He cooling. Results are as follows:

$$L_{\text{copper}} = 1.35 \text{ m}$$

$$L_{\text{HTSC}} = 0.66 \text{ m}$$

$$L_{\text{total}} = 2.65 \text{ m (incl. ends)}$$

$$\dot{m} = 2.35 \text{ g/s}$$

The conductor temperature at the coil end was fixed at 5 K, and the helium temperature was 60 K. Conductor temperature at the warm end with Neumann condition $dT/dx=0$ was 295 K, and the corresponding helium temperature was 290 K. The upper end of the HTSC part was 70 K.

At lower currents, i.e., below 20 kA, the current lead is not more optimized because of the fixed length of the copper conductor.

In Figure 16, the conductor temperature along the current lead is plotted for different currents.

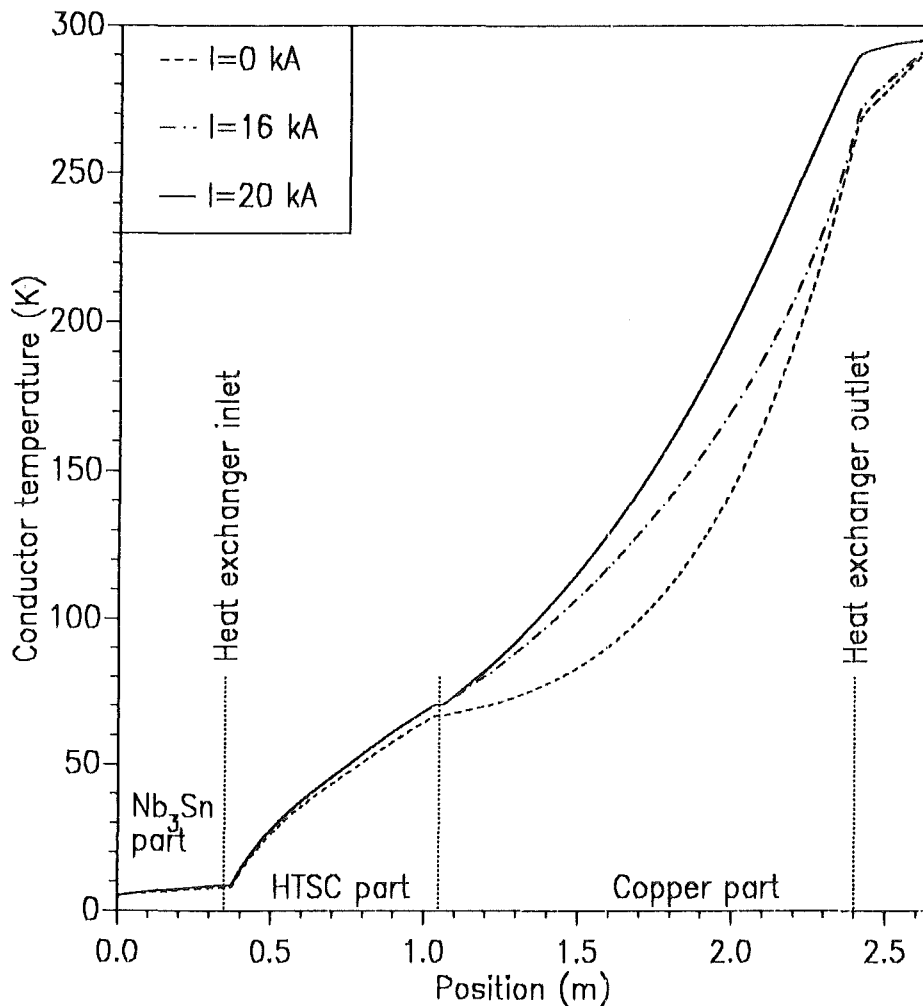


Figure 16. Temperature profiles of HTSC current lead for 60-K He cooling and 0, 16 and 20 kA

There are several conclusions:

- At 20 kA, no heat is conducted toward or out of the warm end of the lead, i.e., the optimization is fulfilled.

- At lower currents, and moreover at zero current, there is a positive temperature gradient at the warm end, resulting in heat flowing toward the lead; i.e., the lead is too short. This leads to a mass flow rate that is larger than for an optimized lead at that current.
- The heat load at the connection region between the HTSC part and the superconducting coil is the sum of the thermal conduction from the HTSC part and the resistive heat of the contact. Therefore, heat load at this location depends on the current.
- The heat load at the connection region between the HTSC part and the copper heat exchanger is the sum of the thermal conduction from the copper heat exchanger and the resistive heat of the connection. Therefore, heat load at this location also depends on current. Due to the temperature difference between the conductor and the helium at the lower end of the copper heat exchanger, the heat load at that location can be partly transferred to the coolant and not conducted to the 4-K level of the lead. As an example for the 20-kA run: heat of about 44 W is conducted from the copper heat exchanger; only 0.5 W is transferred to the HTSC part of the lead, while the main part (i.e., about 99%) is taken by the helium at the lower part of the copper heat exchanger. At the connection area, there is a resistive heat of 6.1 W plus a thermal conduction load of 0.5 W adding to 6.6 W (i.e., these 6.6 W are conducted towards the 4-K level). Table 3 summarizes the heat load results for the various currents.

Current [kA]	4-K level		60-K level	
	Q_{Resi} [W]	Q_{Cond} [W]	Q_{Resi} [W]	Q_{Cond} [W]
0	0.0	6.14	0.0	6.14
6.7	0.21	6.31	0.63	5.67
13.	0.79	6.59	2.79	4.06
16.	1.17	6.71	3.90	2.78
20.	1.87	6.67	6.09	0.57

Table 3. Heat loads at 4-K resp. 60-K level for different currents for 60-K He cooling (version 2)

Figures 17 - 20 show the helium mass flow rate, the mass flow rate normalized to current, the voltage drop, and the maximum temperature of the HTSC as well as the maximum temperature difference between the HTSC part and the helium at the HTSC part as a function of current. The voltage drop, shown in Figure 19, is parabolic, because at higher currents the temperature throughout the entire lead rises with increasing current, and so the resistance in the upper part is somewhat higher. The heat sink at the upper end of the HTSC part is not completely realized because the temperature varies between 66 K and 70 K. But however, the mass flow rate could be adjusted thus to get the same temperature as the HTSC part. In the same way as temperature, the temperature difference between the HTSC and the helium varies.

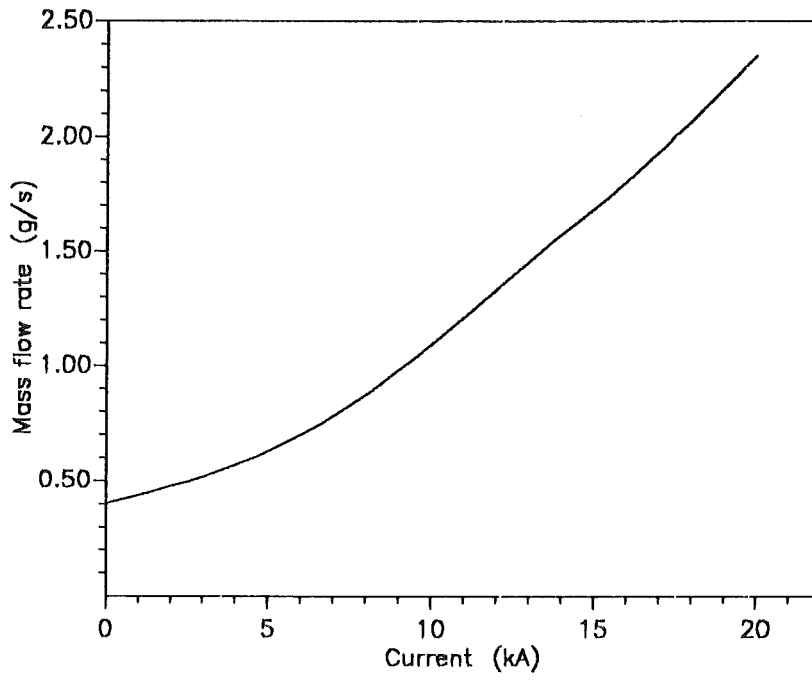


Figure 17. Helium mass flow rate vs. current for 60-K He cooling concept

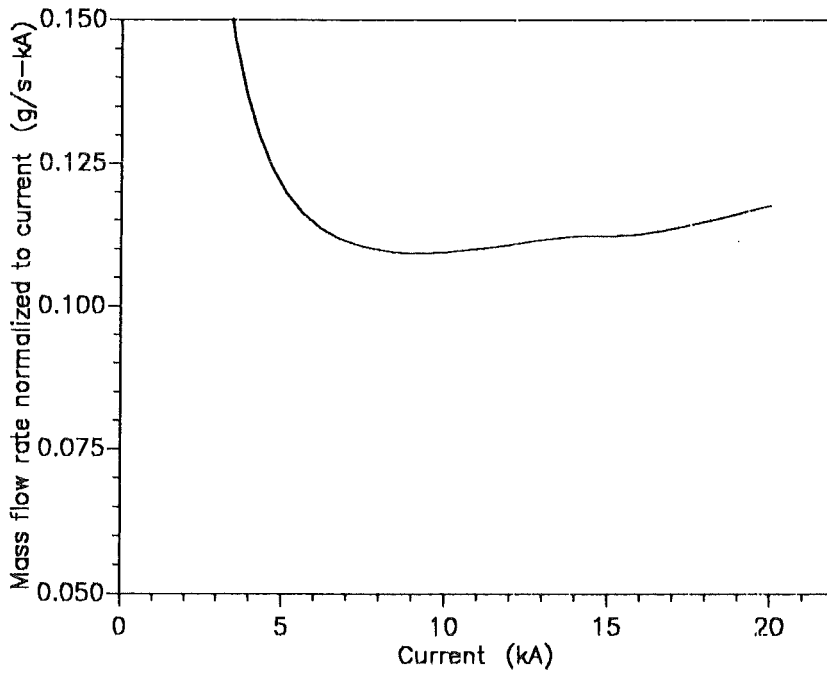


Figure 18. Helium mass flow rate normalized to current vs. current for 60-K He cooling concept

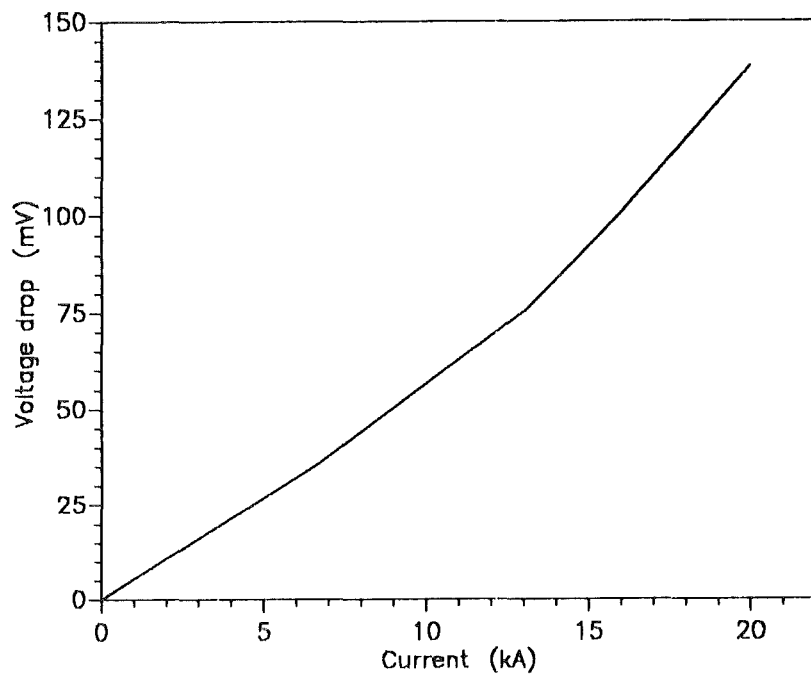


Figure 19. Voltage drop vs. current for 60-K He cooling concept

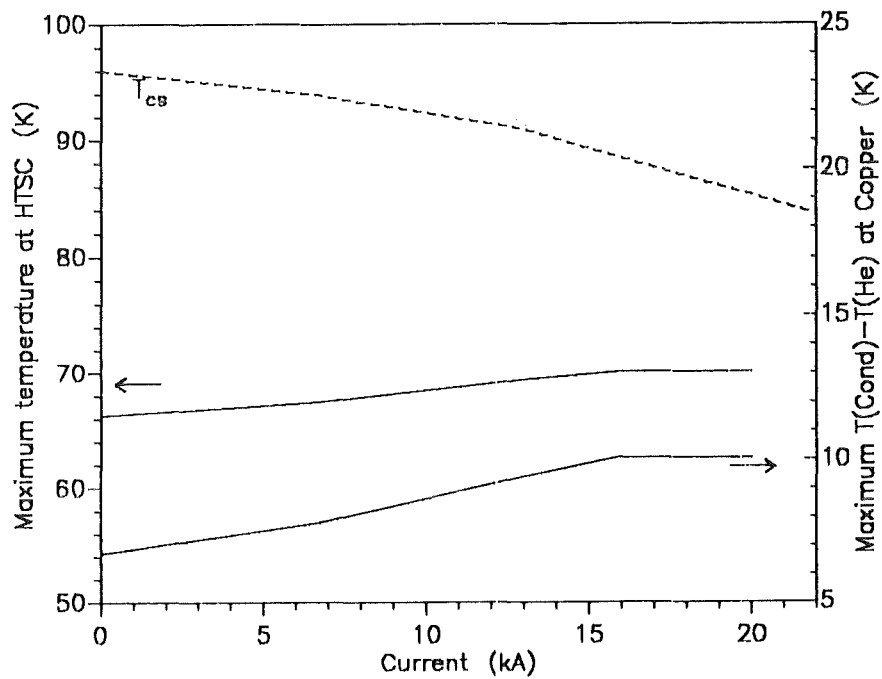


Figure 20. Temperature at upper end of HTSC part and maximum temperature difference between Cu and helium vs. current for 60-K He cooling concept

4.4 Refrigeration power consumption

Based on the results presented above, neither of the cooling concepts has a clear advantage over the other.

Both concepts are discussed here with respect to refrigeration power consumption because this was the main reason for introducing HTSC into the current lead design.

To give a complete picture, one must distinguish between recooling and refrigeration consumption, i.e., the refrigeration power needed for current leads and for superconducting coils. The power rate to cool a lead is related to recooling whereas that for cooling a coil is related to refrigeration.

For calculation of power consumption, the following relations have been used:

Recooling:

$$4.5 \text{ K: } P_w = \dot{m} \cdot [T_0 \cdot \Delta S - \Delta H] = \dot{m} \cdot 6886 \text{ J/g}$$

$$60 \text{ K: } P_w = \dot{m} \cdot [T_0 \cdot \Delta S - \Delta H] = \dot{m} \cdot 1343 \text{ J/g}$$

where

P_w = power consumption at room temperature (293 K),

\dot{m} = mass flow rate,

T_0 = Lower temperature, i.e. 4.5 K resp. 60 K,

ΔS = entropy difference between room temperature and 4.5 K resp. 60 K, and

ΔH = enthalpy difference between room temperature and 4.5 K resp. 60 K.

Refrigeration:

$$4.5 \text{ K: } P_w = 352 \text{ W/W} \cdot P_c$$

where

P_c = power consumption at 4.5 K,

P_w = power consumption at room temperature (293 K).

The individual P_w must be divided by the electrical refrigerator efficiencies. For a 4-K refrigerator, an efficiency factor 0.2 has been used, whereas for a 60-K refrigerator, a factor of 0.3 has been assumed.

With these numbers, the power consumptions for the HTSC lead with 4-K and 60-K He cooling have been computed, together with the numbers for the combined lead. The results are given in Table 4; numbers for recooling and refrigeration are separated in the table.

Current [kA]	Combined lead		HTSC (4-K He)		HTSC (60-K He)	
	Refriger- ation [kW]	Recooling [kW]	Refriger- ation [kW]	Recooling [kW]	Refriger- ation [kW]	Recooling [kW]
0	0.17	6.35	0.81	13.73	2.16	1.79
6.7	0.09	13.74	1.13	14.42	2.3	3.56
13	0.38	24.03	1.57	17.17	2.6	6.49
16	0.55	28.84	1.92	19.23	2.77	8.06
20	0.87	36.39	1.82	23.69	3.0	10.52

Table 4. Recooling and refrigeration rates for various current leads

The main results are:

- The recooling power for the HTSC lead is strongly reduced in 60-K He cooling. This is due to the higher efficiency.
- The refrigeration power for the HTSC lead is greater than for the combined lead, although a contact resistance of 6 nΩ was used in the calculations (see [14]). The reason is that heat conduction is negligible for currents larger than zero because of the Nb₃Sn insert.
- For total power consumption, both power rates must be added.

In Figure 21, total power consumption of the three leads has been plotted for different currents.

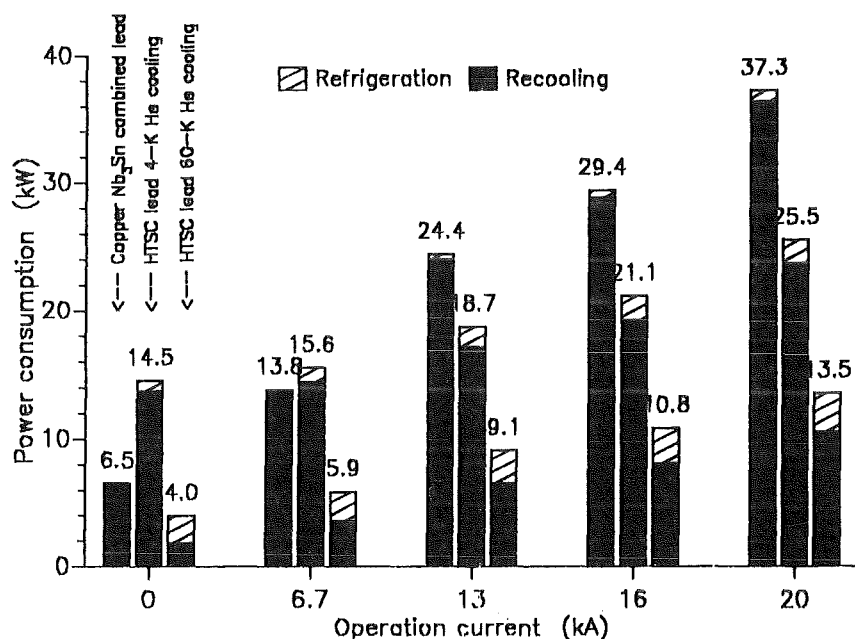


Figure 21. Total power consumptions for the HTSC and the combined leads at different currents

Figure 22 show the percentage of power reduction of the two HTSC leads compared to the combined lead. The upper plot contains only the reduction factor for recooling, which shows an (almost) constant number of about 72% due to the heat sink at the 70-K level. But it is also seen that losses on the 4-K level (refrigeration) reduce the power reduction factor. At higher currents, this is about 10% and at zero current about 40%.

The results clearly show that compared with a conventional lead, the 60-K He cooling concept has the higher refrigeration power reduction. The percentage reduction is essentially independent on current. Thus showing the superiority of this design.

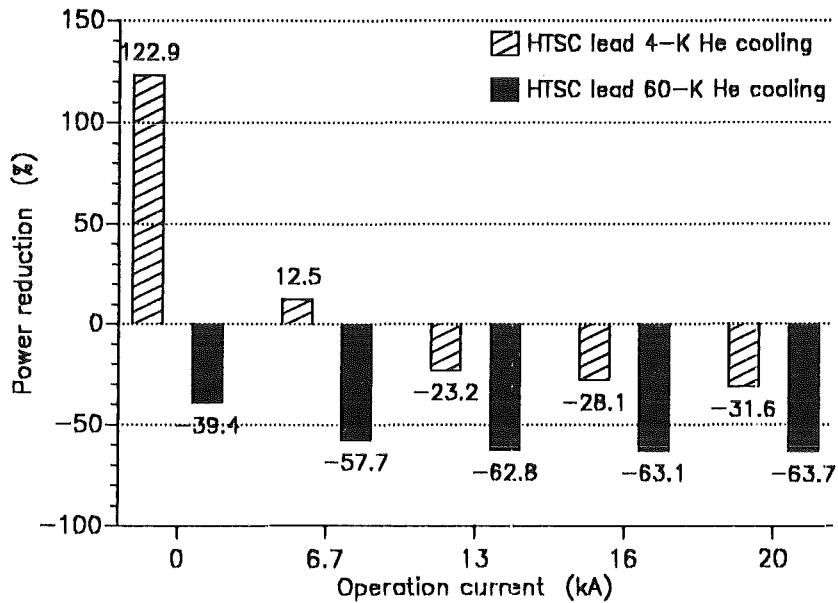
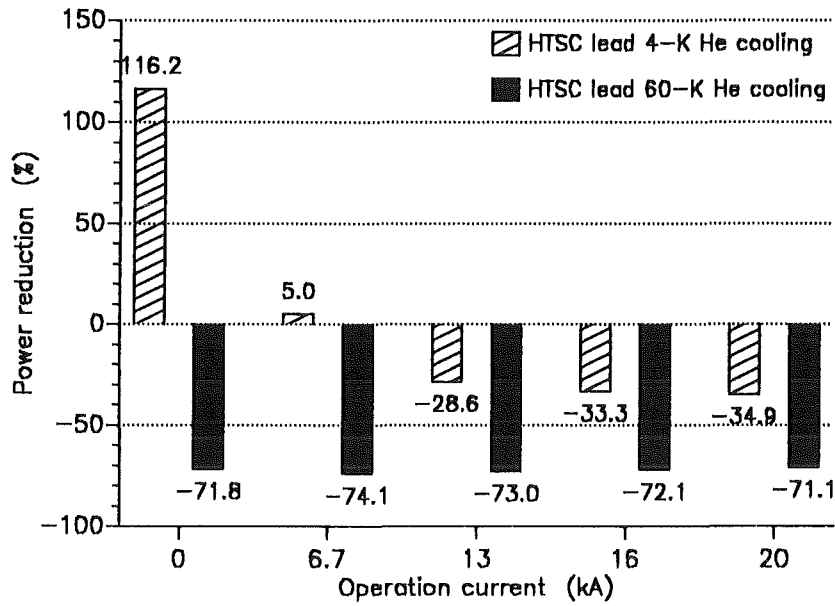


Figure 22. Reduction factor for the HTSC lead for both cooling concepts at different currents.

Top: Only recooling.

Bottom: Recooling and refrigeration.

The conclusion is that the 60-K He cooling concept reduces total refrigeration power more than the 4-K He cooling concept. The refrigeration rate depends on contact losses at the 4-K level; therefore these must be reduced as much as possible. Refrigeration rates also depend on the conduction losses between the 70-K and the 4-K level, which can be reduced only by increasing the length of the HTSC part.

4.5 Effect of contact resistance at 4-K and 60-K levels

For 60-K He cooling, the effect of different contact resistances on the 4-K, as well as on the 60-K level has been studied for a current of 20 kA. A constant mass flow rate of 2.35 g/s has been used in the calculations. Table 5 summarizes the results.

$R_{\text{Clamping,4-K}}$ [nΩ]	$R_{\text{HTSC,4-K}}$ [nΩ]	$R_{\text{HTSC,60-K}}$ [nΩ]	4-K level		60-K level	
			Q_{Resi} [W]	Q_{Cond} [W]	Q_{Resi} [W]	Q_{Cond} [W]
2.5	2.2	15.2	1.87	6.67	6.09	0.57
2.5	2.2	22.4	1.87	6.75	8.96	-2.21
2.5	2.2	31.6	1.87	6.85	12.63	-5.78
2.5	2.2	115.6	1.87	8.01	46.25	-38.24
2.5	4.6	15.2	2.83	6.66	6.09	0.55
2.5	13.5	15.2	6.41	6.59	6.09	0.48

Table 5. Heat loads at 4-K resp. 60-K level for different currents for 60-K He cooling (version 2)

Results of increase of resistance at 60-K level:

Because the temperature at the upper end of the HTSC part increases to 78 K if resistance is increased at the 60-K level by one order of magnitude, the heat conducted from the copper heat exchanger changes the sign. This means that the copper heat exchanger takes most of the heat generated at the contact. The rest is conducted to the 4-K level via the HTSC. Also, the temperature at the warm end of the lead increases because the helium temperature also increases.

Results of increase of resistance at 4-K level:

The heat generated at the 4-K level does not change the heat conducted from the 60-K level via the HTSC but increases the heat load. This result, of course, is the same as for a conventional lead.

Therefore, for power consumption reasons, resistance at the 4-K level should be kept as low as possible whereas resistance at the 60-K level affects mainly the temperature at that location because of the heat exchanger effect.

4.6 Effect of higher temperature of HTSC part

For the 60-K He cooling, the effect of a higher temperature at the upper end of the HTSC part has been studied for a current of 20 kA and different temperatures $T_{HTSC,top}$. The length and the mass flow rate of the copper heat exchanger has been optimized. In Table 6, the main results are summarized.

$T_{HTSC,top}$ [K]	L_{Cu} (L_{HTSC}) [m]	\dot{m} [g/s]	$Q_{cond,4-K}$ [W]	$Q_{cond,60-K}$ [W]	Recool- ing [kW]	Refrig- eration [kW]	Re- duction factor [%]
70	1.35 (0.66)	2.35	6.67	0.57	3.01	10.52	-63.7
77	1.0 (0.66)	1.90	7.92	0.29	3.45	8.51	-67.8
77	1.0 (0.86)	1.90	6.16	-1.58	2.83	8.51	-69.6
90.9	0.77 (1.06)	1.65	6.37	-4.08	2.90	7.39	-72.4

Table 6. Comparison of current leads with different temperatures at the upper end of HTSC part for 60-K He cooling

The main result is that an increase of temperature of the upper end of the HTSC part reduces the recooling rate but enlarges the losses on the 4-K level. To reduce the 4-K heat load, the length of the HTSC part was increased, resulting in a decrease of the 4-K heat load (see Table 6).

It should be mentioned that an increase of $T_{HTSC,top}$ leads to a decrease of the temperature margin, i.e., it reduces the stability of the lead.

Figure 23 shows temperature profiles of the leads with various values of $T_{HTSC,top}$. The subchart shows the corresponding temperature profiles of the HTSC part.

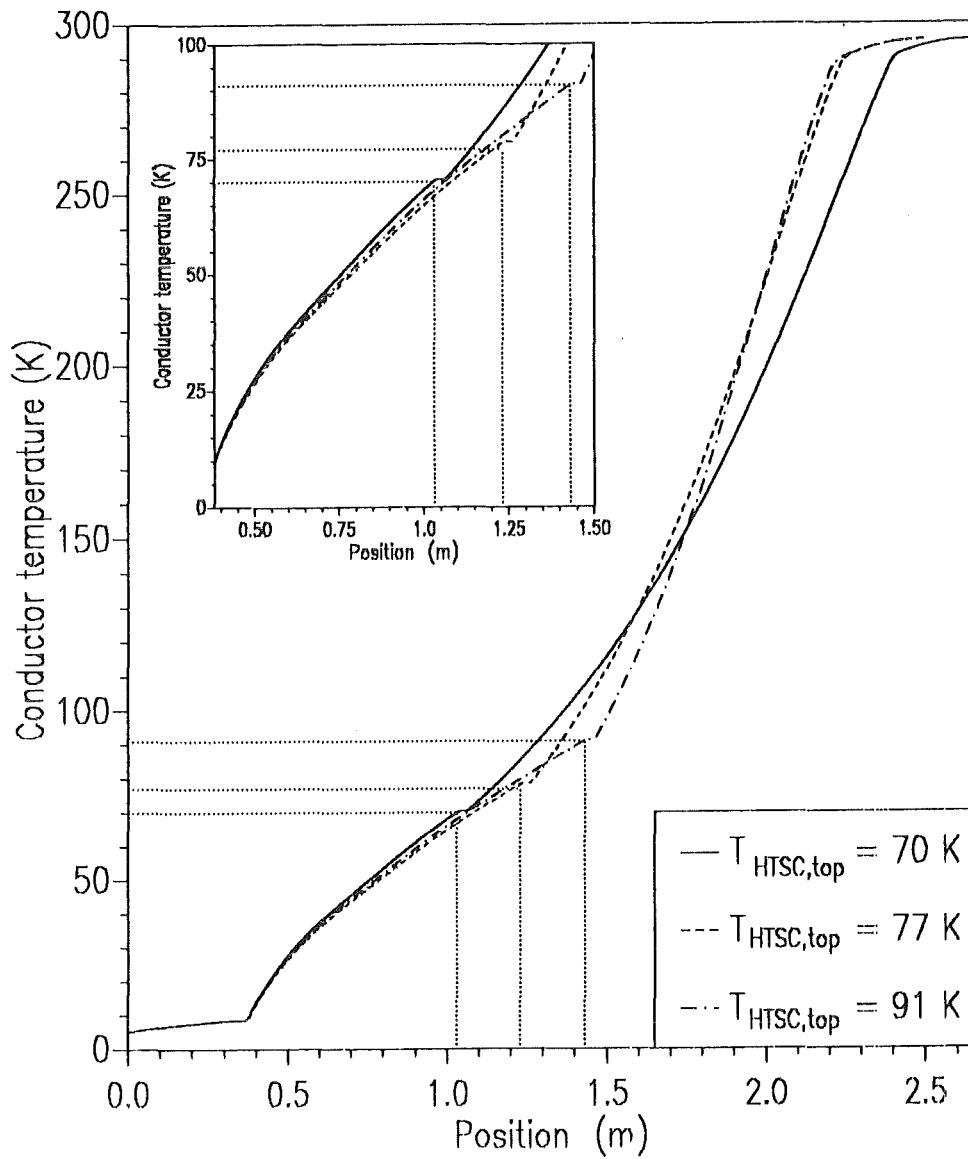


Figure 23. Temperature profiles of HTSC current lead for 60-K He cooling and various temperature at the upper end of HTSC part. Dashed line represents temperature profile for $T_{HTSC,top} = 77$ K, the solid line the corresponding one for $T_{HTSC,top} = 70$ K. Subchart shows temperature profile of HTSC part.

5.0 Transient behaviour in case of loss of helium mass flow

One important feature of a lead is its behaviour in case of loss of coolant flow, which can occur during an experiment if, for example, the circulation pump stops. In case of HTSC, the critical temperature was set to 150°C because the connection between the HTSC and the copper parts were made by soft-soldering. The time to reach this temperature is called the "critical time".

Therefore, the behaviour of the lead was studied numerically for both cooling concepts and an operation current of 20 kA; due to the different geometries, the results could be different.

Starting from the steady-state solution of the current lead at 20 kA, the helium mass flow was set to zero, and the temperature profiles were computed as a function of time. Figure 24 shows the temperature distributions of the lead for the 4-K He cooling concept at different times after switching off the mass flow. Figure 25 shows the results of the lead for the 60-K He cooling concept.

The result shows a different behaviour than that for a lead where the HTSC part consists of bulk superconductor [7]:

1. The critical time is much larger, i.e., in our case it is more than 5 min. For a rough design using bulk HTSC, even with a lower current density of 2.9 A/mm², the burn-out time, i.e., the time to reach 700 K, was only about 1 min.
2. There is no hot spot as for bulk HTSC, although there is a peak region in the HTSC part of the lead. This is indeed a substantial difference from a combined copper lead and results from the lower thermal conductivity and the higher electrical resistivity of the HTSC. But the effect of the Ag-alloy stabilizer can be clearly seen by looking in Figure 26. There, the same calculation was done without Ag-alloy stabilizer. The result is that after about 13 s, there is a hot spot near to the upper end of the HTSC part of the lead.
3. The broadening of the high-temperature region results in an increase of the temperature of the connection area at the coil side after 4 min (60-K He cooling - version 2) and 5 min (4-K He cooling - version 1). This also indicates the thermally stabilizing effect of the Ag alloy. There is an interplay between the amount of temperature increase in the HTSC part and at the coil side. There seem to be two extreme cases: the copper lead with no hot-spot region and the bulk HTSC lead with no increase of 4-K heat load.
4. When the mass flow stops, there are several minutes before either the "critical time" is reached or the temperature at the bottom of the lead begins to rise. Thus there is ample time to de-energize most magnets before the lead is damaged and before the magnet quenches.

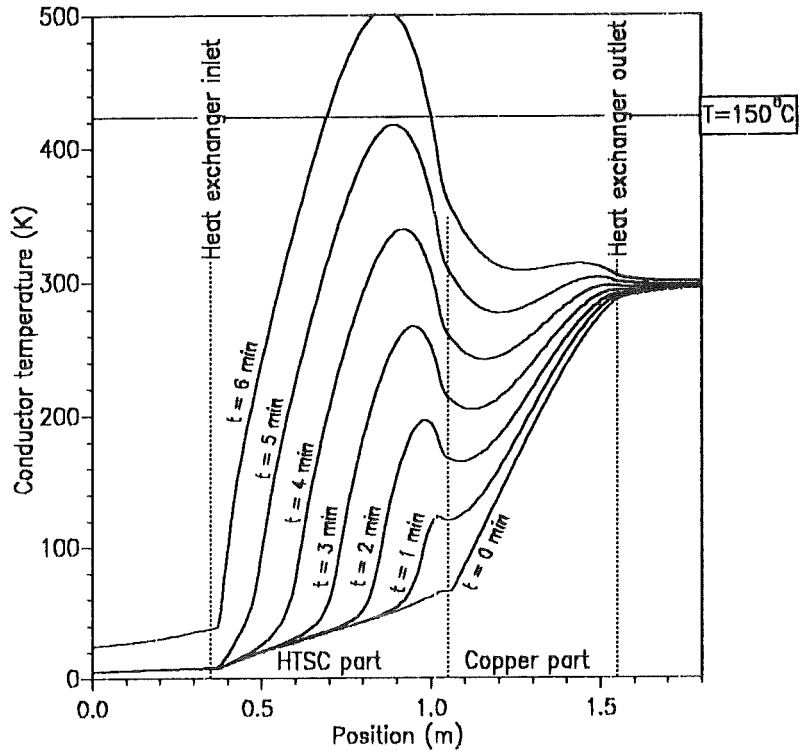


Figure 24. Temperature profiles of HTSC lead at 20 kA at various times after switching off helium mass flow (4-K He cooling)

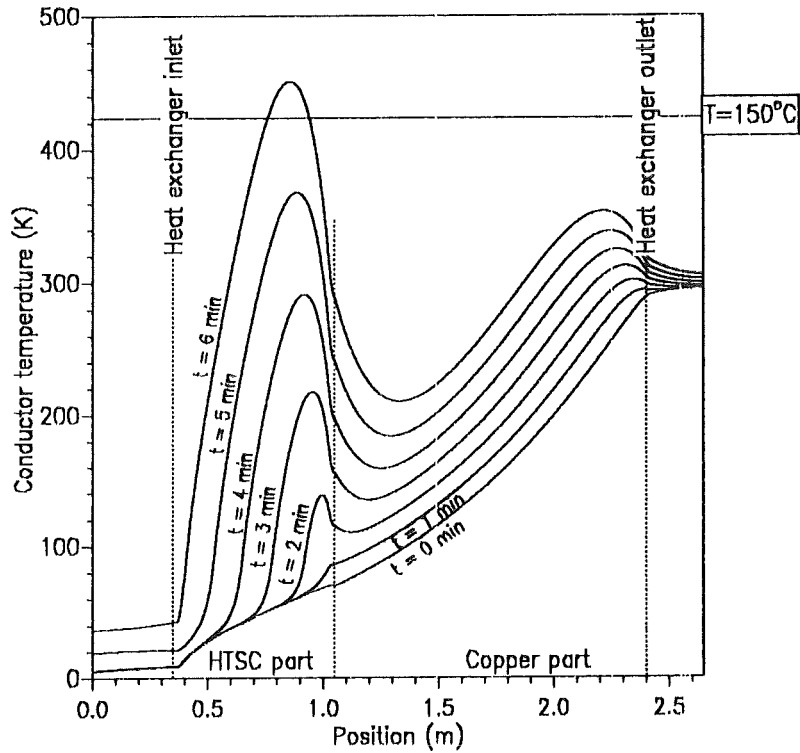


Figure 25. Temperature profiles of HTSC lead at 20 kA at various times after switching off helium mass flow (60-K He cooling)

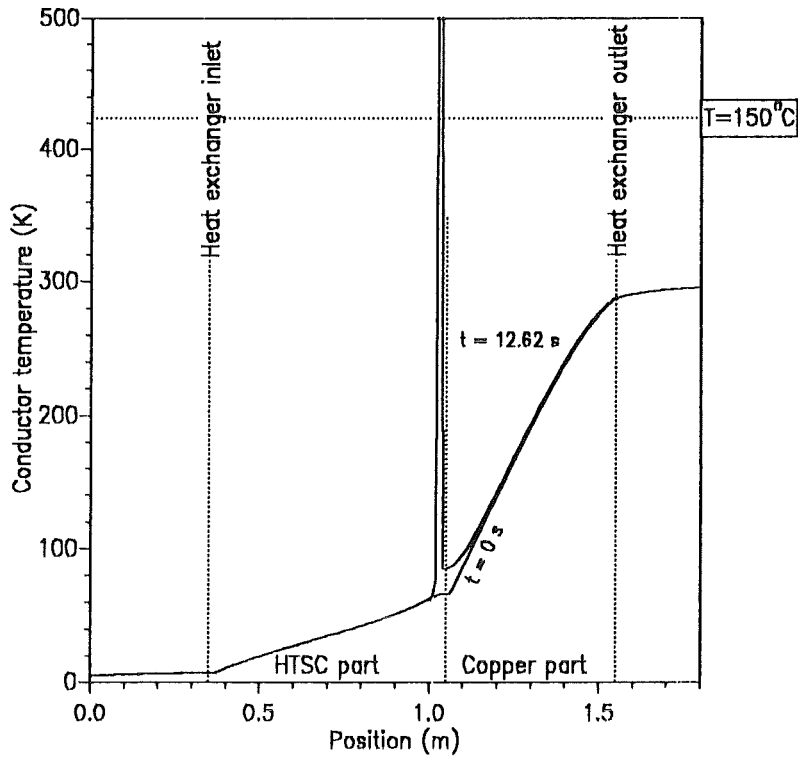


Figure 26. Temperature profiles of HTSC lead at 20 kA without Ag-alloy stabilizer after switching off helium mass flow (4-K He cooling)

These results led to the question of the amount of stabilizer needed in that design to balance in time the thermal load to the coil and the hot-spot region within the HTSC. Therefore, calculations were done by starting again from the steady-state solution of the lead for the 4-K He cooling concept and varying the cross section of the Ag alloy by keeping the HTSC area constant. Then the mass flow was stopped, and the temperature profiles were computed up to the time-of-danger. In Figure 27, the time-of-danger is plotted as a function of the Ag-alloy stabilizer fraction in the HTSC part of the lead. In the same figure, the temperature at the coil side of the lead at the same time is shown, too. The current lead design values are indicated as solid circles.

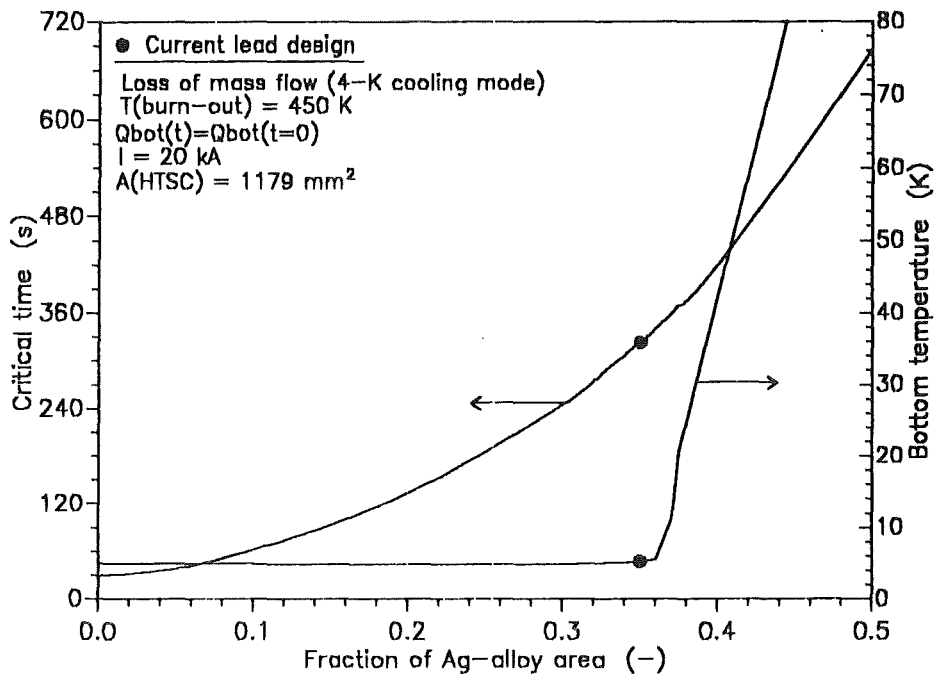


Figure 27. Critical time and temperature at coil side (bottom temperature) of HTSC lead at 20 kA after switching off mass flow (4-K He cooling). Design values are indicated in the figure.

Obviously, the design is nearly at the point where the two effects discussed above will coincide.

Figure 28 shows the temperature profiles for the different stabilized HTSC leads. If the Ag-alloy stabilizer cross section is increased, the hot-spot peak broadens and grows slower.

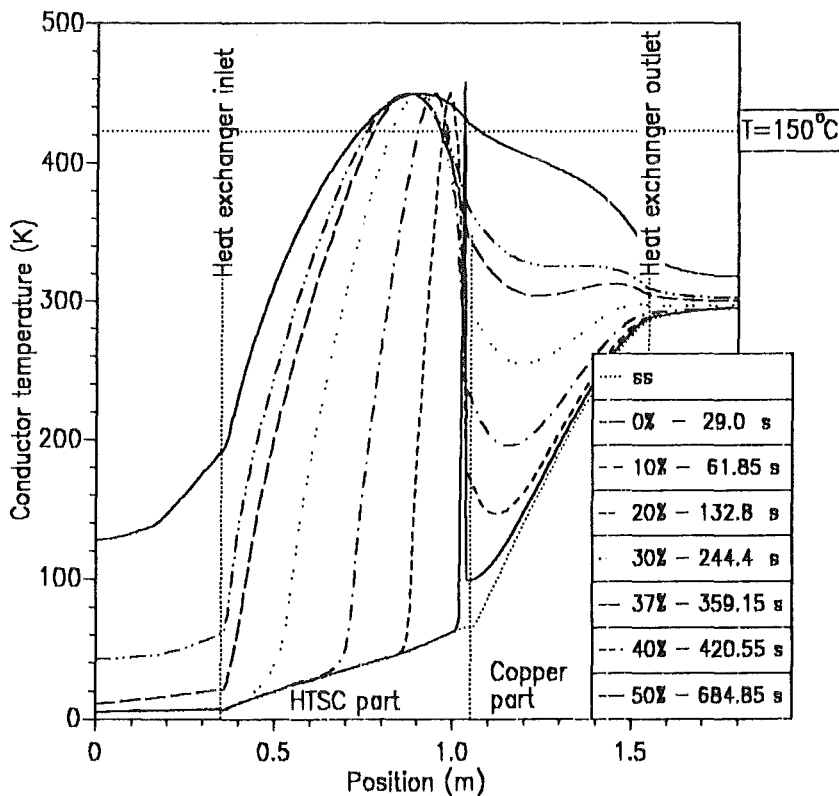


Figure 28. Temperature profiles of HTSC lead at 20 kA for different Ag-alloy stabilizer cross sections at the burn-out time (4-K He cooling). Design values are indicated in the figure.

6.0 Summary and conclusions

A conceptual design for a 20-kA current lead consists of an HTSC part and a copper heat exchanger. The HTSC part is built up of Bi-2223 tapes stabilized with Ag-alloy sheaths. Bi-2223 tapes have been used because of their higher critical current density in applied medium magnetic fields.

The higher thermal conductivity of the HTSC tapes requires longer lengths for current lead application as bulk material, i.e., 0.66 m instead of 0.20 m. Because of the higher critical current density, the cross section of the HTSC part is smaller than of the copper heat exchanger conductor, i.e., 18.14 cm² instead of 28.3 cm². For current leads built with HTSC bulk material having critical current densities of less than 1 A/mm², we would have a cross section of 200 cm². This would lead to heat loads being higher than for design presented using HTSC tapes: the heat load for Bi-2223 tapes sheathed with Ag-Au alloy is about 2 W whereas for Bi-2212 bulk material between 4 K and 70 K it is about 7 W.

Two cooling concepts were discussed with respect to refrigerator power consumption and compared to a 16-kA current lead design proposed for the planned stellarator W 7-X, i.e., the 4-K He and the 60-K He cooling. If both recooling and refrigeration power are considered, 4-K He cooling reduces the power consumption to 70% of its original values, whereas 60-K He cooling reduces it to 36%.

For 60-K He cooling, the effect of increasing contact resistances at the 4-K and 60-K levels are studied: the critical number is the resistance at the 4-K level because it directly changes the heat load and therefore the refrigeration rate. Resistance at the 60-K level has only a minor effect.

For 60-K He cooling, the increase in temperature at the upper end of the HTSC part has been studied: An increase of $T_{HTSC,top}$ leads to a decrease of the mass flow rate and therefore of the recooling rate. To get no increase of heat load at the 4-K level as well as the refrigeration rate, the length of the HTSC part must be increased. It should be noted that the temperature margin is reduced if $T_{HTSC,top}$ increases, this may affect the thermal stability of the lead.

The use of Ag-alloy-sheathed Bi-2223 tapes has a second advantage: it reduces the danger of creating a hot spot in the HTSC part in case of loss of mass flow. If the HTSC quenches due to temperature increase, the sheath can carry the current for some time, and the higher thermal conductivity distributes the heat in a larger volume. Both facts increase the time for reaching the critical temperature, which is determined by the melting temperature of the soft solder used in the design. Here, we obtained a time of more than 4 min after interruption of mass flow. This is ample time to de-energize most magnets before the lead is damaged and before the magnet quenches.

The results obtained in the design study allow extrapolation to leads operating in the 50 kA regime, i.e., those planned for use in ITER.

Acknowledgement

Work at KfK has been performed within the frame of the European Fusion Technology Programme. Work at ANL was supported by the U.S. Department of Energy, Energy Efficiency and Renewable Energy, as part of a program to develop electric power technology, under Contract W-31-109-Eng-38.

7.0 References

- [1] J.R. Hull, "High temperature superconducting current lead," IEEE Trans. on Appl. Supercond., Vol. 3, No. 1 (1993) 869-875
- [2] R. Wesche and A.M. Fuchs, "Design of superconducting current leads," Cryogenics 34, No. 2 (1994) 145-155
A.M. Fuchs et al., "Development of Binary Superconducting Current Leads With a Gas Cooled Normal Part," presented at Int. Cryog. Eng. Conf. ICEC-15, 7.-10. June Genova
- [3] R.C. Niemann et al., "High Temperature Superconducting Current Leads for Micro-SMES Application," IEEE Trans. on Magn. (1994), 2589-2592
- [4] K. Ueda et al., "Thermal Performance of a Pair of Current Leads Incorporating Bismuth Compound Superconductors," Adv. in Supercond. V (1993), 1235-1238
- [5] P.F. Herrmann et al., "Test results of a 1 kA (2 kA)-20 kV HTSC current lead model," Cryogenics 34 (6) (1994), 543-548
- [6] O.F. Herrmann et al., "European project for the development of high T_c current leads," presented at 1992 Applied Superconductivity Conference - August 23-28, 1992, Chicago
- [7] R. Heller, "Numerical study of a 50 kA Current Lead Using Bulk High Temperature Superconductors," KfK 5172 (1993)
- [8] H. Fujishiro et al., "Low Thermal Conductive Bi-2223 Tapes Sheathed with Ag-Au Alloys," To be published in IEEE Trans. on Magn. (1994)
- [9] T. Sasoka et al., "Characteristics of Ag-Au alloy sheathed Bi-Pb-Sr-Ca-Cu-O superconducting tapes for current leads," Appl. Phys. Lett. 64 (10) (1994), 1304-1305
- [10] J. Kessler, "Präparation und supraleitende Eigenschaften von Bi(2212)-Drähten und Bi(2223)-Bändern mit Ag- und dispersionsgehärteten AgMgO-Hüllen," Thesis, University of Karlsruhe (1993), unpublished
- [11] G. Grasso et al., "Critical current densities and their field dependence in long, rolled Bi(2223) tapes," presented at CIMTEC, Florence, Italy, June 1994
- [12] C. Beidler et al., "Physics and engineering design for Wendelstein 7-X," Report IPP 2/300 (1989)
- [13] R. Heller et al., "Test of a Forced-Flow Cooled 30 kA / 23 kV Current Lead for the POLO Model Coil," to be published in IEEE Trans. on Magn. (1994)
- [14] R. Heller, report, Kernforschungszentrum Karlsruhe, (1993) unpublished
- [15] G. Friesinger and R. Heller, "Use of Nb_3Sn inserts in a forced flow cooled 30 kA current lead," Appl. Supercond. Vol. 2, No. 1 (1994)
- [16] S.J. Sackett, "EFFI, a code for calculating the electromagnetic field, force and inductance in coil systems of arbitrary geometry," LLNL, Livermore, California, UCRL-52402 (1978)
- [17] T. Kato et al., "development of 10 kA-class go & return high- T_c superconducting bus bar," paper presented at the ISS 93 (1993)
- [18] R. Heller, "Numerical calculation of current leads for fusion magnets," KfK 4608 (1989)
- [19] R. Heller and C. Rieger, report, Kernforschungszentrum Karlsruhe, (1992) unpublished